



**HAL**  
open science

# Dynamical approximations for composite quantum systems: Assessment of error estimates for a separable ansatz

Irene Burghardt, Rémi Carles, Clotilde Fermanian Kammerer, Benjamin Lasorne, Caroline Lasser

## ► To cite this version:

Irene Burghardt, Rémi Carles, Clotilde Fermanian Kammerer, Benjamin Lasorne, Caroline Lasser. Dynamical approximations for composite quantum systems: Assessment of error estimates for a separable ansatz. 2021. hal-03868449v1

**HAL Id: hal-03868449**

**<https://hal.science/hal-03868449v1>**

Preprint submitted on 9 Dec 2021 (v1), last revised 23 Nov 2022 (v3)

**HAL** is a multi-disciplinary open access archive for the deposit and dissemination of scientific research documents, whether they are published or not. The documents may come from teaching and research institutions in France or abroad, or from public or private research centers.

L'archive ouverte pluridisciplinaire **HAL**, est destinée au dépôt et à la diffusion de documents scientifiques de niveau recherche, publiés ou non, émanant des établissements d'enseignement et de recherche français ou étrangers, des laboratoires publics ou privés.

# DYNAMICAL APPROXIMATIONS FOR COMPOSITE QUANTUM SYSTEMS: ASSESSMENT OF ERROR ESTIMATES FOR A SEPARABLE ANSATZ

IRENE BURGHARDT, RÉMI CARLES, CLOTILDE FERMANIAN KAMMERER,  
BENJAMIN LASORNE, AND CAROLINE LASSER

ABSTRACT. Numerical studies are presented to assess error estimates for a separable (Hartree) approximation for dynamically evolving composite quantum systems which exhibit distinct scales defined by their mass and frequency ratios. The relevant error estimates were formally described in our previous work [I. Burghardt, R. Carles, C. Fermanian Kammerer, B. Lasorne, C. Lasser, J. Phys. A. 54, 414002 (2021)]. Specifically, we consider a representative two-dimensional tunneling system where a double well and a harmonic coordinate are cubically coupled. The time-dependent Hartree approximation is compared with a fully correlated solution, for different parameter regimes. The impact of the coupling and the resulting correlations are quantitatively assessed in terms of a time-dependent reaction probability along the tunneling coordinate. We show that the numerical error is correctly predicted on moderate time scales by a theoretically derived error estimate.

## 1. INTRODUCTION

The time-dependent Hartree (TDH) approximation, also termed time-dependent self-consistent field method [5, 7, 8], which represents the time propagation of composite quantum systems within a separable (Hartree) approximation, is ubiquitous in quantum and classical-statistical physics. This approximation is based on a mean-field description and often works well if the relevant subspaces are weakly coupled, and if a separation of scales is given due to disparities in mass and/or frequency. The TDH approximation is also a natural starting point for including correlations in terms of sums of products, i.e., using a correlated multiconfigurational (MC) ansatz that leads to a Multiconfiguration Time-Dependent Hartree (MCTDH) [13, 1] form of the wavefunction. Related tensor representations of multidimensional wavefunctions are cast in the form of matrix product states [17, 18]. A variational setting [1, 12] is generally employed to obtain generalized, multiconfigurational mean-field equations for such correlated wavefunctions. The TDH and MCTDH representations can be straightforwardly adapted to fermionic or

---

*Key words and phrases.* Scale separation, composite quantum systems, quantum dynamics, quantum tunneling, system-bath theory, dimension reduction.

bosonic systems. In the present context, we refer to distinguishable particles for simplicity.

Despite the importance of the TDH ansatz, an explicit error analysis of this approach is not often reported in the literature. In a recent formal paper [3], we therefore presented error estimates for the time propagation of composite quantum systems within the TDH approximation. We also compared different types of approximate product wavefunctions, i.e., based on Taylor expansion (collocation) or else on the TDH mean-field approach, and we further considered a semiclassical approximation within a quantum-classical type treatment. In the present paper, we follow up on this previous work and carry out numerical simulations to assess the previously derived error estimates for a realistic, anharmonically coupled system exhibiting a separation of scales defined by the relevant mass and frequency ratios. As in the formal paper mentioned above, the present study is meant to be a first step towards a general analysis of scale separation in the context of multiconfigurational, tensorized wavefunction representations.

Specifically, we consider numerical simulations for a two-dimensional tunneling system where a double-well potential is anharmonically coupled to a harmonic coordinate. As in Ref. [3], a cubic coupling is considered (i.e., linear in the tunneling coordinate and quadratic in the harmonic coordinate). Numerical TDH calculations for different parameter regimes are compared with correlated MCTDH calculations that can be considered as numerically exact for the present system. The impact of the coupling and the resulting correlations are quantitatively assessed in terms of a time-dependent reaction probability along the tunneling coordinate.

A time-dependent error estimate is expressed quantitatively in terms of the relevant parameters of the Hamiltonian, leading to insight into the “small” parameters to be considered to gauge the validity of the TDH approximation. This leads us to question the conventional viewpoint that mass ratios are decisive; indeed, within our present analysis, it is the frequency ratio that is found to play a more important role.

The paper is organized as follows. Section 2 presents the model Hamiltonian under consideration and gives a detailed account of the relevant parameters and their scaling properties. Section 3 addresses the TDH approximation and Section 4 details the formulation of time-dependent error estimates. Section 5 presents the numerical results and Section 6 concludes.

## 2. MODEL SYSTEM

In line with our previous work [3], we consider a two-dimensional model system which is of system-bath type and exhibits anharmonicities both within the system subspace and in the system-bath coupling. Specifically, a double-well potential is chosen in the system subspace, which is coupled to a harmonic bath coordinate *via* a cubic (quadratic times linear) coupling term. As pointed out in our previous analysis [3], a cubic coupling is a non-trivial

case which is relevant for the description of vibrational dephasing [11, 9] and Fermi resonances [2] in a molecular physics context.

**2.1. Hamiltonian in physical scaling.** In system-bath form, the Hamiltonian is written as follows,

$$\mathcal{H} = H_X + H_Y + W(X, Y),$$

with the subspace Hamiltonians

$$H_X = -\frac{\hbar^2}{2\mu_1}\Delta_X + V_1(X), \quad H_Y = -\frac{\hbar^2}{2\mu_2}\Delta_Y + V_2(Y),$$

where  $V_1(X)$  corresponds to a double-well potential and  $V_2(Y)$  is a harmonic form,

$$V_1(X) = \frac{k_1^0}{2} X^2 \left( \frac{X}{2L} - 1 \right)^2, \quad V_2(Y) = \frac{1}{2}k_2^0 Y^2.$$

The system potential  $V_1(X)$  represents a symmetric double well with two equivalent minima at  $X = 0$  and  $X = 2L$  that can be taken to correspond to the “reactant” vs. “product” in the context of a reactive process [14]. The energy at the barrier  $X = L$  amounts to  $D_1 = k_1^0 L^2/8$ .

The coupling  $W(X, Y)$  is given as a cubic term, i.e., linear in  $X$  and quadratic in  $Y$ ,

$$W(X, Y) = \frac{1}{2}\eta^0 XY^2.$$

Viewed from a different angle,  $V_2(Y)$  and  $W(X, Y)$  can be combined into an effective potential for the  $Y$  coordinate,

$$V_2^{\text{eff}} = V_2(Y) + W(X, Y) = \frac{1}{2}(k_2^0 + \eta^0 X) Y^2 \equiv \frac{1}{2}k_2(X) Y^2,$$

whose curvature is  $X$ -dependent, i.e., the local force constant is given as  $k_2(X) = k_2^0 + \eta^0 X$ . We denote the ratio of the curvature along  $Y$ , taken at the product versus reactant minima in  $X$ , by

$$(1) \quad \alpha = \frac{k_2(X = 2L)}{k_2(X = 0)} = 1 + 2\frac{\eta^0}{k_2^0}L.$$

The reduced parameter  $\alpha$  gives a direct measure of the relative coupling strength upon characterizing how much the local curvature for  $Y$  changes as  $X$  varies from 0 (reactant minimum) to  $2L$  (product minimum).

Yet from a different perspective, an adiabatic regime can be considered whose “fast” subsystem ( $X$ ) coordinate is coupled to a “slow” bath ( $Y$ ) coordinate. An effective subsystem Hamiltonian can then be defined as follows,

$$H_1^{\text{eff}} = -\frac{\hbar^2}{2\mu_1}\Delta_X + V(X, Y) \quad V(X, Y) = V_1(X) + V_2(Y) + W(X, Y).$$

Which perspective is most appropriate depends on the physical time scales under study, as will be detailed below.

Finally, we note that the extension of this model to multivariate coordinates  $X$  and  $Y$  is straightforward, such that the present model is suitable to address general multidimensional tunneling situations.

**2.2. Parameter choice.** In the present work, we exclusively consider negative values of the coupling parameter  $\eta^0$  such that the curvature ratio defined in Eq. (1) satisfies  $\alpha < 1$ . This ensures that the ground eigenstate of the full  $(X, Y)$ -system is localized around the product well ( $X = 2L > 0$ ), while nonstationary dynamics will start from an initial condition (or, in mathematical language, an initial datum) localized around the reactant well ( $X = 0$ ). In other words, we reverse localization in order to create an initial nonstationary state.

The cubic coupling potential  $W(X, Y)$  has to be handled with some care. It causes the potential energy to be unbounded from below beyond the controllable subquadratic regime. This is likely to induce numerical issues and renders the Hamiltonian  $H$  only formally self-adjoint. One might therefore either add a contribution to the potential energy that is quartically confining with respect to  $Y$  or multiply the coupling potential with a cut-off function in  $X$ . Here we have chosen another simple approach: There exists a critical value  $X = X_c = \frac{2L}{1-\alpha} > 0$  where  $k_2(X = X_c) = 0$ , which is called a valley-ridge inflection point [10]. Despite its relevance in terms of bifurcation aspects, this is not the situation that we want to address here. A simple cure is to ensure that such a critical point occurs far enough from  $X = 2L$  that the potential energy at this point,  $V(X = X_c, Y = 0) = V_1(X_c)$ , is large enough compared to the barrier height,  $D_1 = k_1^0 L^2/8$ . As will be shown below, we choose our reference model such that  $\alpha = \frac{1}{3}$  and  $X_c = 3L$ , which implies that  $V_1(X_c)$  is nine times larger than  $D_1$ . The most “precarious” case we considered is  $\alpha = \frac{1}{4}$  and  $X_c = \frac{8L}{3}$ , which implies that we have  $V_1(X_c) = \frac{256}{81}D_1 \approx 3.2D_1$ . Such a range of values for the onset of unboundedness in the potential energy seems *a priori* far enough that our low-energy wavepackets will be vanishing in critical regions, which is what we also observed in practice.

**2.3. Representation in scaled coordinates.** In order to transform the Hamiltonian to a suitably scaled representation, we introduce the (angular) frequencies and the corresponding natural length scales of the harmonic approximations for  $X$  and  $Y$  around the origin,

$$\omega_i^0 = \sqrt{k_i^0/\mu_i}, \quad a_i^0 = \sqrt{\hbar/(\mu_i\omega_i^0)}$$

for  $i = 1, 2$ . The corresponding natural energy and time scales are

$$E_i^0 = \frac{\hbar^2}{\mu_i(a_i^0)^2} = k_i^0(a_i^0)^2 = \hbar\omega_i^0, \quad t_i^0 = \frac{\hbar}{E_i^0}.$$

Note that, *e.g.*,  $\{\mu_1, a_1^0, t_1^0\}$  can serve as a consistent and complete set of mechanical units for all quantities built on powers of [M][L][T], whereby  $\hbar$

is numerically equal to unity due to the relationship between the energy unit  $E_1^0$  and the time unit  $t_1^0$  (much as when considering atomic units). In the spirit of semiclassical scaling, we further introduce a typical parameter defined as the square root of the mass ratios,

$$\varepsilon = \sqrt{\frac{\mu_1}{\mu_2}}.$$

Scaling both coordinates with respect to the natural length scale of the system coordinate, while the bath coordinate is additionally scaled by  $\varepsilon$ , we set

$$(x, y) = \left( \frac{1}{a_1^0} X, \frac{1}{a_1^0 \varepsilon} Y \right), \quad \ell = \frac{L}{a_1^0}.$$

We thus obtain a scaled Hamiltonian

$$\mathcal{H} = E_1^0 H,$$

where the dimensionless part reads

$$H = -\frac{1}{2} \Delta_x - \frac{1}{2} \Delta_y + v(x, y),$$

with potential energy

$$v(x, y) = v_1(x) + v_2(y) + w(x, y),$$

with contributions from the system (double well) and the harmonic bath mode

$$v_1(x) = \frac{1}{2} x^2 \left( \frac{x}{2\ell} - 1 \right)^2, \quad v_2(y) = \frac{1}{2} \varpi^2 y^2,$$

where  $\varpi = \omega_2^0 / \omega_1^0$  denotes the frequency ratio of the bath versus the system. The coupling potential  $w(x, y) = \frac{1}{2} \eta x y^2$  features the rescaled coupling constant

$$\eta = \frac{(a_1^0)^3 \varepsilon^2}{E_1^0} \eta^0.$$

Let us denote the physical time  $T$  and the rescaled time  $t$ , where

$$t = \frac{T}{t_1^0} = \frac{E_1^0}{\hbar} T.$$

We can absorb both  $E_1^0$  and  $\hbar$  into  $t_1^0$  and recast the time-dependent Schrödinger equation,

$$i\hbar \partial_T \Psi(T, X, Y) = \mathcal{H} \Psi(T, X, Y),$$

into dimensionless form as

$$i\partial_t \psi(t, x, y) = H \psi(t, x, y).$$

We observe that the curvature ratio defined in Eq. (1) is invariant under the performed linear coordinate scaling. It is related to the coupling constant according to

$$\alpha = 1 + 2 \frac{\eta}{\varpi^2} \ell \quad \text{resp.} \quad \eta = \varpi^2 \frac{\alpha - 1}{2\ell}.$$

The parametrization in terms of the frequency ratio  $\varpi$  and the curvature ratio  $\alpha$  fully characterizes the interaction of the system and bath via the potential energy. The parameter  $\varepsilon$ , which represents the mass ratio, only appears indirectly, through the scaling of the  $Y$  coordinate and of the  $\eta$  parameter.

**2.4. Relevant parameter regime and initial data.** In view of the numerical simulation results reported below, we now specify the parameter regime which was considered in these simulations. First, a reference model was constructed by the following choice of parameters,

$$\varepsilon_* = \frac{1}{4}, \quad \varpi_* = \frac{1}{100}, \quad \alpha_* = \frac{1}{3}.$$

We note that the mass ratio  $\varepsilon_*$  is moderate, but representative of chemically relevant systems. The frequency ratio  $\varpi_*$ , however, takes a larger value, and will be demonstrated to play an important role in the error estimates to be discussed below.

In the simulations reported below, we explore the dynamics of several variations of this reference model (i.e., cases 0 to 8, while the reference model is denoted case \*, see Table 1). Relevant ranges of values for  $\alpha$  have been discussed above. As already pointed out, reducing  $\alpha$  below values of about  $\frac{1}{4}$  could entail issues related to the unboundedness within the space explored by the wavepacket. Note also that “case 3” appeared in our simulations as the most sensitive situation, bringing much larger errors between correlated and uncorrelated descriptions. We suspect that this may reflect the fact that the corresponding time scale of the  $Y$  dynamics, now shorter, enters the realm of the time scale of  $X$  motion (see Sec. 5 for further discussion), thus making system-bath separability less justified.

In all cases, we chose the initial data to be the approximate Gaussian quasi-coherent ground state localized in the “reactant well”, as illustrated in Fig. 1,

$$(2) \quad \psi(t = 0, x, y) = \chi_0(x)\phi_0(y) = (2\pi)^{-1/2}\varpi^{-1/4} \exp\left(-\frac{1}{2}x^2 - \frac{\varpi}{2}y^2\right).$$

The squeezing in the  $y$  direction, due to the  $\varpi$  factor in the coherent state width, reflects that this coordinate tends towards the classical limit.

### 3. TIME-DEPENDENT HARTREE APPROXIMATION

We compare the numerical solution of the full Schrödinger equation with separable, normalized initial datum

$$\begin{cases} i\partial_t\psi(t, x, y) = H\psi(t, x, y), \\ \psi(t = 0, x, y) = \chi_0(x)\phi_0(y), \end{cases}$$

with the one of the TDH approximation subject to the same initial condition,

$$\begin{cases} i\partial_t u(t, x, y) = H_u^{\text{eff}}(t)u(t, x, y), \\ u(t = 0, x, y) = \chi_0(x)\phi_0(y). \end{cases}$$

Case	$\varepsilon$	$\varpi$	$\alpha$	
*	$\varepsilon_*$	$\varpi_*$	$\alpha_*$	reference
0	$\varepsilon_*$	$\varpi_*$	1	no coupling
1	$2\varepsilon_*$	$\varpi_*$	$\alpha_*$	
2	$\frac{1}{2}\varepsilon_*$	$\varpi_*$	$\alpha_*$	
3	$\varepsilon_*$	$4\varpi_*$	$\alpha_*$	most sensitive
4	$\varepsilon_*$	$\frac{1}{4}\varpi_*$	$\alpha_*$	
5	$\varepsilon_*$	$\varpi_*$	$\frac{3}{4}\alpha_*$	
6	$\varepsilon_*$	$\varpi_*$	$\frac{3}{2}\alpha_*$	
7	$\varepsilon_*$	$\varpi_*$	$2\alpha_*$	
8	$\varepsilon_*$	$\varpi_*$	$\frac{9}{4}\alpha_*$	

TABLE 1. Parameter variations of the reference model, that is defined by the values  $(\varepsilon_*, \varpi_*, \alpha_*) = (\frac{1}{4}, \frac{1}{100}, \frac{1}{3})$ . These parameters determine the square root of the mass ratio, the frequency ratio, and the curvature ratio, respectively.

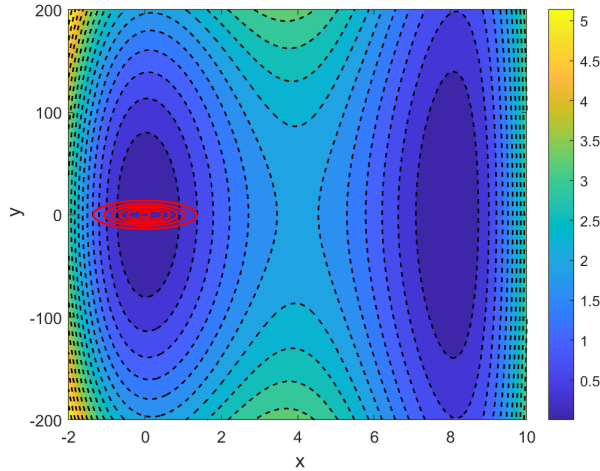


FIGURE 1. Contour plot of the two-dimensional potential energy surface and coherent-state initial condition according to Eq. (2). As explained in the text, the initial condition corresponds to a non-stationary state localized in the less stable left (“reactant”) well.

The effective TDH Hamiltonian

$$H_u^{\text{eff}}(t) = \langle H \rangle_\phi^{(x)}(t) + \langle H \rangle_\chi^{(y)}(t) - \langle H \rangle_u(t),$$

is additive with respect to the coordinates and thus preserves the product structure of the initial datum, i.e., we have

$$u(t, x, y) = a(t) \chi(t, x) \phi(t, y),$$

where  $a(t)$  is a complex number of absolute value one, acting as a suitably chosen gauge factor. The individual product wavefunctions satisfy the coupled equations of motion

$$\begin{aligned} i\partial_t\chi(t, x) &= \langle H \rangle_\phi(t)\chi(t, x), \\ i\partial_t\phi(t, y) &= \langle H \rangle_\chi(t)\phi(t, y), \end{aligned}$$

while the gauge factor

$$a(t) = \exp\left(i \int_0^t \langle H \rangle_u(s) ds\right)$$

depends on the full energy expectation with respect to the Hartree product. Our system-bath type Hamiltonian is of the form

$$H = H_x + H_y + w(x, y),$$

with  $H_x = -\frac{1}{2}\Delta_x + v_1(x)$  and  $H_y = -\frac{1}{2}\Delta_y + v_2(y)$ . In this situation, the effective Hartree Hamiltonian is of the form

$$H_u^{\text{eff}}(t) = H_x + H_y + w_u^{\text{eff}}(t, x, y),$$

and differs from the true Hamiltonian only with respect to the effective coupling potential

$$(3) \quad w_u^{\text{eff}}(t, x, y) = \langle w \rangle_\phi(t, x) + \langle w \rangle_\chi(t, y) - \langle w \rangle_u(t),$$

so the above effective Hamiltonians can be rewritten as

$$\langle H \rangle_\phi = H_x + \langle w \rangle_\phi(t, x), \quad \langle H \rangle_\chi = H_y + \langle w \rangle_\chi(t, y).$$

#### 4. ERROR ESTIMATES

For analyzing the approximation error

$$e(t, x, y) = \psi(t, x, y) - u(t, x, y),$$

we use a standard stability estimate, see Lemma 2 in Ref. [3] Differentiating the error with respect to time we obtain a Schrödinger-type equation

$$\begin{cases} i\partial_t e(t, x, y) = H e(t, x, y) + \Sigma_u(t, x, y), \\ e(t=0, x, y) = 0, \end{cases}$$

with source term

$$\Sigma_u(t, x, y) = (H - H_u^{\text{eff}}(t)) u(t, x, y) = (w(x, y) - w_u^{\text{eff}}(t, x, y)) u(t, x, y).$$

By the variation of constants formula (aka the Duhamel principle), we write the error as a time-integral,

$$(4) \quad e(t, x, y) = \frac{1}{i} \int_0^t \exp(-iH(t-s)) \Sigma_u(s, x, y) ds.$$

Since the time-evolution associated with the Hamiltonian  $H$  is unitary, we now estimate

$$\|e(t)\|_{L^2} \leq \int_0^t \|\Sigma_u(s)\|_{L^2} ds$$

for the  $L^2$ -norm of the error.

**4.1. Formula for the source term.** The cubic coupling potential of our system-bath type Hamiltonian is of product form

$$w(x, y) = w_1(x)w_2(y).$$

Therefore, the coupling potential of the Hartree approximation, see Eq. (3), takes the special form

$$w_u^{\text{eff}}(t, x, y) = w_1(x) \langle w_2 \rangle_\phi(t) + \langle w_1 \rangle_\chi(t) w_2(y) - \langle w_1 \rangle_\chi(t) \langle w_2 \rangle_\phi(t).$$

This implies for the difference of the coupling potentials

$$\begin{aligned} \delta w_u(t, x, y) &= w(x, y) - w_u^{\text{eff}}(t, x, y) \\ &= (w_1(x) - \langle w_1 \rangle_\chi(t)) (w_2(y) - \langle w_2 \rangle_\phi(t)). \end{aligned}$$

We provide a detailed computation of the local-in-time error given in Example 3 of Ref. [3]. We calculate the norm of the source term  $\Sigma_u(t) = \delta w_u(t)u(t)$  according to

$$\begin{aligned} \|\Sigma_u(t)\|_{L^2}^2 &= \langle \delta w^2 \rangle_u(t) \\ &= \left\langle [w_1(x) - \langle w_1 \rangle_\chi(t)]^2 \right\rangle_\chi \left\langle [w_2(y) - \langle w_2 \rangle_\phi(t)]^2 \right\rangle_\phi \\ &= (\langle w_1^2 \rangle_\chi(t) - \langle w_1 \rangle_\chi(t)^2) (\langle w_2^2 \rangle_\phi(t) - \langle w_2 \rangle_\phi(t)^2). \end{aligned}$$

From a probabilistic point of view, we can interpret this formula as the product of the variances of  $w_1$  and  $w_2$ . Applying this formula to the cubic coupling model, we then obtain the error estimate

$$\|\psi(t) - u(t)\|_{L^2} \leq \frac{1}{2} |\eta| \int_0^t \sqrt{(\langle x^2 \rangle_\chi(s) - \langle x \rangle_\chi^2(s)) (\langle y^4 \rangle_\phi(s) - \langle y^2 \rangle_\phi^2(s))} ds.$$

**4.2. Dimension analysis.** This formula is given here in terms of dimensionless energy, space, and time variables; its proof is not affected by scaling considerations, and it directly translates into physical units,  $(X, Y, T)$ , as

$$\begin{aligned} &\|\Psi(T) - U(T)\|_{L^2} \leq \frac{1}{2} |\eta^0| \times \\ (5) \quad &\frac{1}{\hbar} \int_0^T \sqrt{(\langle X^2 \rangle_X(S) - \langle X \rangle_X^2(S)) (\langle Y^4 \rangle_Y(S) - \langle Y^2 \rangle_Y^2(S))} dS. \end{aligned}$$

From  $\eta^0 = \frac{E_1^0}{(a_1^0)^3 \varepsilon^2} \eta$ , recalling  $E_1^0 = \frac{\hbar}{t_1^0}$ , and  $\eta = \varpi^2 \varsigma$ , where

$$\varsigma = \frac{\alpha - 1}{2\ell},$$

the upper bound of the previous estimate can be recast in terms of dimensionless ratios as

$$\begin{aligned} & \frac{\varpi^2|\varsigma|}{2t_1^0} \int_0^T \sqrt{\frac{\langle X^2 \rangle_X(S) - \langle X \rangle_X^2(S)}{(a_1^0)^2} \frac{\langle Y^4 \rangle_Y(S) - \langle Y^2 \rangle_Y^2(S)}{\epsilon^4 (a_1^0)^4}} dS \\ &= \frac{\varpi^2|\varsigma|}{2t_1^0} \int_0^T \sqrt{\frac{\langle X^2 \rangle_X(S) - \langle X \rangle_X^2(S)}{(a_1^0)^2} \frac{\langle Y^4 \rangle_Y(S) - \langle Y^2 \rangle_Y^2(S)}{\varpi^2 (a_2^0)^4}} dS \\ &= \frac{\varpi|\varsigma|}{2t_1^0} \int_0^T \sqrt{\frac{\langle X^2 \rangle_X(S) - \langle X \rangle_X^2(S)}{(a_1^0)^2} \frac{\langle Y^4 \rangle_Y(S) - \langle Y^2 \rangle_Y^2(S)}{(a_2^0)^4}} dS, \end{aligned}$$

where we used

$$\frac{a_2^0}{a_1^0} = \frac{\epsilon}{\sqrt{\varpi}},$$

and eliminated the somewhat artificial dependence on  $\epsilon$  (noting that different values of  $\epsilon$  only bring homothetic dynamics with respect to  $Y$ ). As a crucial consequence, we removed one power order of  $\varpi$  regarding natural orders of magnitude and effective “smallness”.

**4.3. Linearization of the upper bound.** From an operational point of view, the purpose of rescaling essentially consists in determining relevant orders of magnitude for the values of the various factors entering the relevant formulae. Since we specifically chose initial data to be quasi-coherent states (within a harmonic approximation around the origin), we know that the product of  $X$  and  $Y^2$  standard deviations expressed in their respective natural units satisfy

$$\sqrt{\frac{\langle X^2 \rangle_X(T=0) - \langle X \rangle_X^2(T=0)}{(a_1^0)^2}} \times \sqrt{\frac{\langle Y^4 \rangle_Y(T=0) - \langle Y^2 \rangle_Y^2(T=0)}{(a_2^0)^4}} = \frac{1}{2},$$

and will not change dramatically over time, which is the incentive for considering a rescaling based on natural units. We can thus further propose a sort of “rough” linear estimate for short times as follows,

$$(6) \quad \|\Psi(T) - U(T)\|_{L^2} \lesssim \frac{1}{4} \varpi |\varsigma| \frac{T}{t_1^0}.$$

where  $\lesssim$  here is to be understood as preceding an approximate upper bound. Such an approximation is not aimed at being precise beyond very short times (although we shall see later on that it works surprisingly well at later times) but it presents the great advantage of providing an easy estimate of relevant orders of magnitude before performing any actual propagation. In the present situation, the initial widths along  $X$  and  $Y$  were chosen to vary as little as possible over time (quasi-coherent initial datum); however, it is not so difficult to make a rough prediction of the time evolution of standard deviations in more general cases (especially oscillatory breathing behaviors with harmonic half periods).

It is worth noticing that *we have identified the prefactor  $\varpi\varsigma = (\eta/\varpi)$  that appears in Eq. (6) as an objective measure of the impact of the coupling on the rate of growth of the error with respect to time.* This was not evident at first sight when starting from  $\eta^0$  as in Eq. (5) written with physical units. It required the dimension analysis presented above so as to get rid of dimensioned quantities and identify what will take values close to unity. The parameter  $\varsigma$  only affects the coupling between the system and the bath but can only be varied moderately. In contrast,  $\varpi$  can span a large range; however, changing its value affects both the coupling and the relative timescales between system and bath.

We also emphasize that the error in the norm of the difference between two normalized wavefunctions is limited by a strict upper bound, a “maximum maximorum”, which is  $\sqrt{2}$  (in the worst and undesired case of strict orthogonality between the solution and its approximation). The intersection of our estimate with this value gives a maximal time of relevance for the estimate, but also a predictive rough order of magnitude of the time beyond which an uncorrelated approximation is definitely at risk.

## 5. RESULTS AND DISCUSSION

All simulations presented below were computed with the Quantics software [19]. Reference simulations denoted as “fully correlated” in the following refer to converged MCTDH calculations where correlated system-bath states are propagated under variational equations of motion [13, 1, 12]. In the specific case of two degrees of freedom, the MCTDH wavefunction ansatz reads as follows, as a generalization of the TDH ansatz,

$$(7) \quad \psi(t, x, y) = \sum_{j_1=1}^n \sum_{j_2=1}^n A_{j_1 j_2}(t) \varphi_{j_1}(t, x) \chi_{j_2}(t, y)$$

The convergence of the multiconfigurational expansion is measured in terms of the so-called natural orbital populations [1]. Typically, expansions up to  $n = 3$  were necessary in order to achieve convergence for the present systems. Related MCTDH calculations for two-dimensional tunneling situations are reported, e.g., in Ref. [15].

**5.1. Characteristic times of dynamical simulations.** For reference, we first consider the uncoupled model (case 0; see Table 1). The characteristics of our model are such that we can distinguish three very different time scales, all separated by two orders of magnitude, for the  $X$  subsystem dynamics: long, short, and medium times. The long time scale  $\sim 100$  ps relates to “ground-state tunneling” (induced by the energy splitting between the ground-state tunneling pair); the medium time scale  $\sim 1$  ps is “excited-state tunneling” (first excited tunneling pair splitting); the short time  $\sim 0.01$  ps is due to “quasiharmonic” motion (vibration around the local minimum).

Our preferred observable for monitoring the dynamics will be the “reaction probability”,  $R(T) = \langle H_L \rangle(T)$ . It is defined as the expectation value

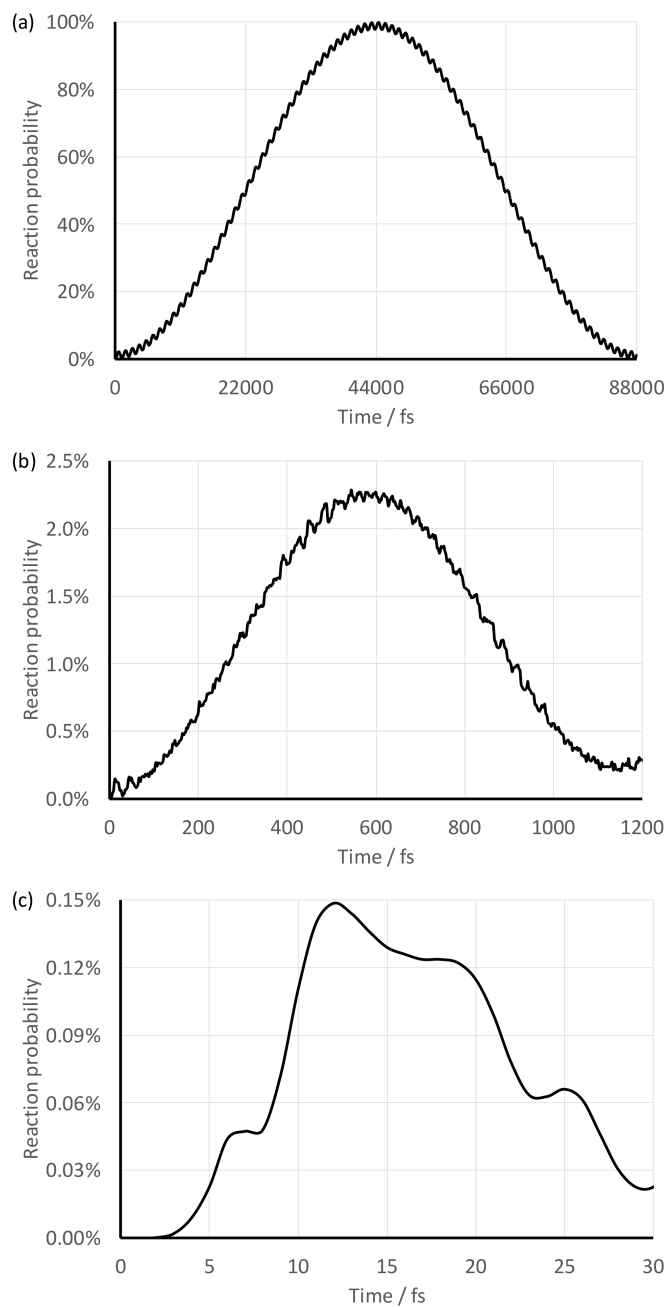


FIGURE 2. Fully correlated (MCTDH) propagation: Time evolution of the reaction probability,  $R(T)$ , in the uncoupled case; (a) long times (ground-state tunneling); (b) medium times (excited-state tunneling); (c) short times (quasiharmonic).

of the Heaviside step distribution centered at  $X = L$ , such that it provides a measure of the probability for the system to be in the product region ( $X > L$ ) at any given time.

In the uncoupled case, the time evolution of  $R(T)$  shows a perfect tunneling quantum beat between the “reactant” ( $X = 0$ ) and “product” ( $X = 2L$ ) wells. It oscillates between about 0 and 1 with a long period of about 88 ps; see Fig. 2. There is a clear modulation (around 2%) with a medium period of about 1.2 ps. One also notices an extra modulation (around 0.1%) with a short pseudoperiod of about 30 fs and even shorter convoluted temporal structures.

These typical times can be rationalized in terms of the eigenstate decomposition of the initial datum, which corresponds almost perfectly (with 49%) to a one-to-one mixture of the even vs. odd members of the ground-state tunneling pair. As a result, the initial wavepacket is localized on the “reactant” side. The corresponding eigenenergies are  $975.92 \text{ cm}^{-1}$  and  $976.30 \text{ cm}^{-1}$  (wavenumbers will be used as customary energy equivalents within this vibrational context). The tunneling energy splitting of  $0.38 \text{ cm}^{-1}$  corresponds to a ground-state tunneling period of 88.0 ps, as indeed observed as reported above (long time scale). Note that the single-well harmonic approximation of the zero-point energy around the origin is at  $1010 \text{ cm}^{-1}$  (the first tunneling pair is redshifted by about  $24 \text{ cm}^{-1}$  due to the anharmonicity of the double well). The initial wavepacket also contains to some extent a contribution of the next tunneling pair with respect to  $X$ : i.e., a 1% component of both members of the excited-state tunneling pair, at  $2728 \text{ cm}^{-1}$  and  $2757 \text{ cm}^{-1}$ , split by  $29 \text{ cm}^{-1}$ . This induces a medium time scale pertaining to the excited tunneling period of 1.2 ps, as indeed observed. The shorter times are more subtle to interpret. The harmonic approximation around the origin (with an energy quantum of  $2000 \text{ cm}^{-1}$ ) would induce a harmonic period of 17 fs. The actual difference between the average eigenenergies of the first two tunneling pairs is a bit lower, at  $1767 \text{ cm}^{-1}$  with a time of 19 fs, on the same order of magnitude as what we identified as a short pseudoperiod of 30 fs, which can be termed a “quasiharmonic” time. The overall dynamics thus appears to be governed by a four-level eigensystem organized as a “pair of pairs”. Note that the harmonic period for  $Y$  is 1.7 ps (with an energy quantum of  $20 \text{ cm}^{-1}$ ), hence, slightly larger than the medium timescale.

Apart from the details of the interpretation, the present setting is ideal for our study, as we are dealing with three typical timescales that are well separated from each other by about two orders of magnitude.

We calculated the reaction probability for all cases given in Table 1. Results for the reference model (\*) and cases 3 and 4 are presented in Fig. 3, for long and medium times both with the fully correlated (MCTDH) and TDH methods. Short-time results are not shown, since these are all virtually identical to the uncoupled case (the dynamics is still uncorrelated).

Upon comparing the left and right panels in Fig. 3, we observe significant differences between fully correlated (MCTDH) and TDH results at long

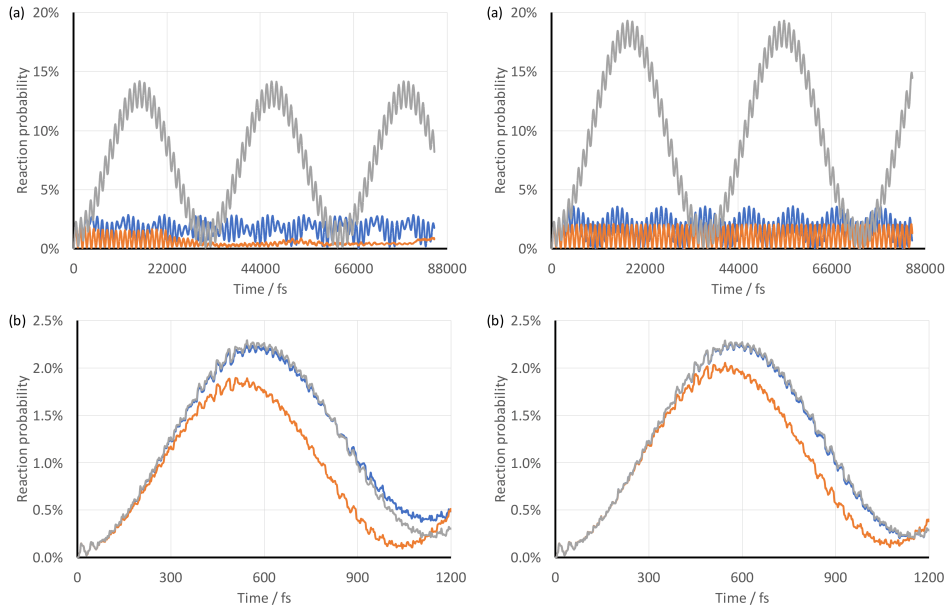


FIGURE 3. Fully correlated (MCTDH) vs. TDH propagation: Time evolution of the reaction probability,  $R(T)$ , in three coupled cases (blue: case 0; orange: case 3; grey: case 4 – see Table 1); the two left panels show fully correlated (MCTDH), the two right panels TDH propagation; (a) long times (ground-state tunneling); (b) medium times (excited-state tunneling).

times: (i) the reaction probabilities obtained with TDH do not experience any oscillation damping as opposed to the fully correlated calculations; (ii) the TDH population transfer is slower (smaller rate); (iii) the net transfer is bigger (larger yield).

From a local comparison in time, the error could be considered as very large. However, from a global perspective, the dynamical behavior is qualitatively similar and the orders of magnitude are correct. For example, taking case 4 (grey curves), the tunneling period is 31 fs (fully correlated) *vs.* 37 fs (TDH) and the rate is 14% (fully correlated) *vs.* 19% (TDH). Let us now turn to a more detailed analysis of the error in the time-dependent wavefunction.

**5.2. Numerical assessment of error estimates.** We calculated the actual norm of the error between fully correlated (MCTDH) and TDH wavepackets at all times,  $\|\Psi(T) - U(T)\|_{L^2}$ , in the seven coupled cases given in Table 1. These are shown in the left panels of Fig. 4. We also calculated the error estimate given in Eq. (5), as well as its linear approximation defined in Eq. (6), see Fig. 5.

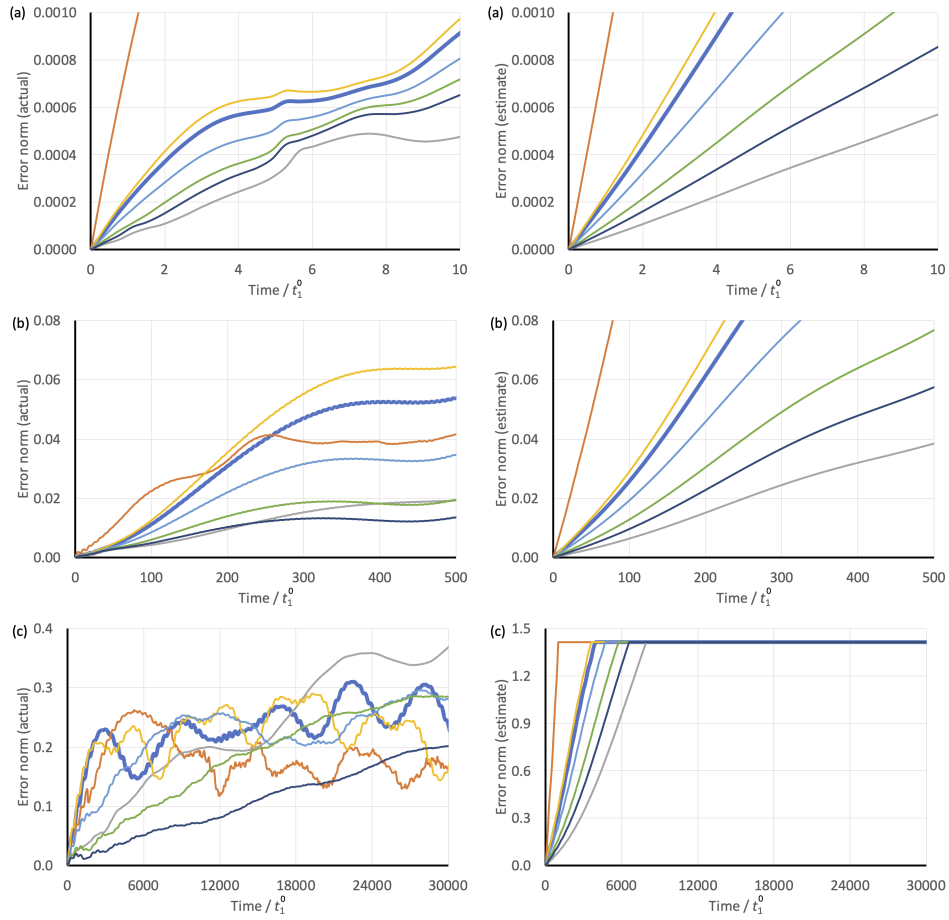


FIGURE 4. Time evolution of the norm  $\|\Psi(T) - U(T)\|_{L^2}$  of the actual error and of the error estimate – see Eq. (5) – in seven coupled cases (thick blue: case 0; orange: case 3; grey: case 4; yellow: case 5; light blue: case 6; green: case 7; dark blue: case 8 – see Table 1); the three left panels show the actual error, the three right ones the estimate; (a) long times; (b) medium times; (c) short times.

The error estimate given in Eq. (5) appears to be almost exact over dimensionless times  $\sim 100 t_1^0$  where  $t_1^0 = 2.65$  fs (natural time for  $X$ ). It is still dominated by a linear growth with time, as illustrated by its strong similarity with its linear approximation (Eq. (6)). The latter stays quite identical to the former up to about  $100 t_1^0$  (compare both panels (b) in Figs 5). This reflects small variations of the various moments, consistent with using a quasi-coherent state as initial datum.

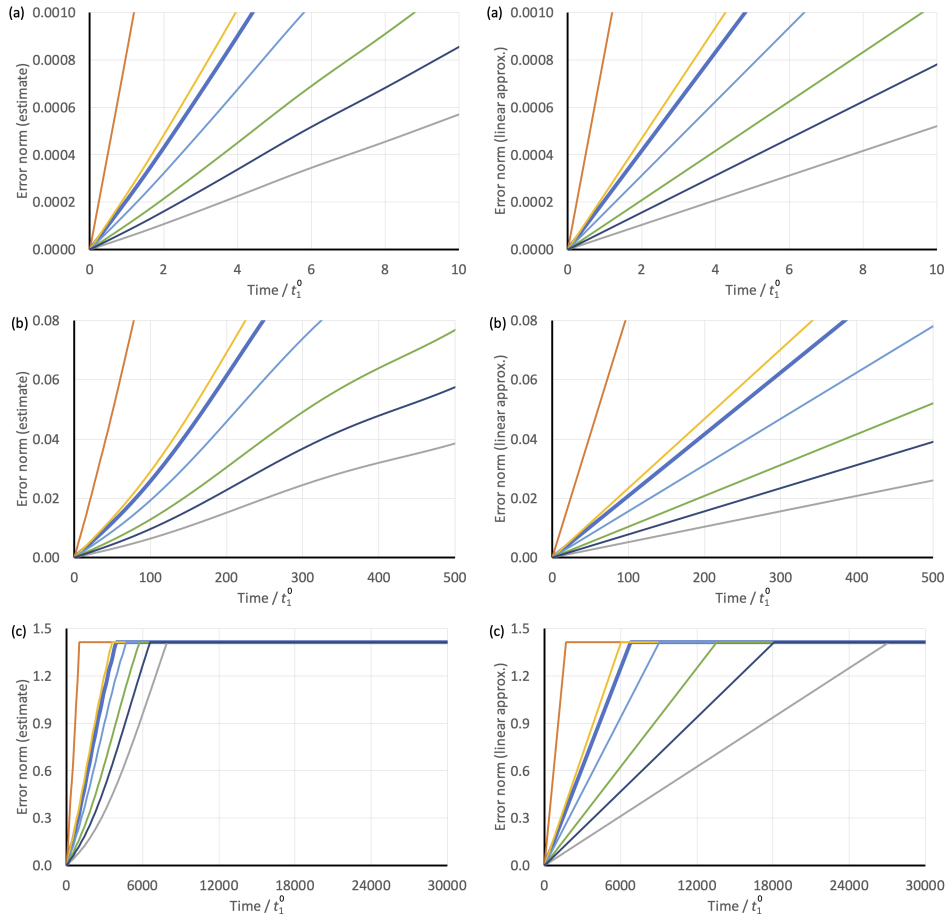


FIGURE 5. Time evolution of the error estimate – see Eq. (5) – and the linear approximation – see Eq. (6) – in seven coupled cases (thick blue: case 0; orange: case 3; grey: case 4; yellow: case 5; light blue: case 6; green: case 7; dark blue: case 8 – see Table 1); the three left panels show the error estimate, the three right ones the linearization; (a) long times; (b) medium times; (c) short times.

Both rigorous and approximate error estimates keep cases ordered over time (no crossing between curves) according to the value of the linear prefactor,  $\varpi\varsigma$ , while the actual error starts to become more complicated, showing various types of oscillations and some rough saturation around 0.2 to 0.3.

Our estimates keep increasing and stop becoming relevant at  $\sim 1000 t_1^0$ ; they still can be viewed as upper bounds, though. Note that they finally lose any significance when they reach the critical value  $\sqrt{2}$ , where orthogonality between the approximate and exact solutions sets in.

## 6. CONCLUSIONS AND OUTLOOK

Following up on the recently presented mathematical framework for error estimation in the context of composite quantum systems [3], we presented here a first application to a non-trivial two-dimensional system where tunneling motion (i.e., a “reactive subsystem”) is coupled to a quasi-harmonic degree of freedom via a cubic coupling. Parameters were chosen to correspond to realistic molecular situations, while allowing for significant quantum effects, within a tunneling process that exhibits three characteristic time scales.

For reference, the reliability of a separable time-dependent Hartree ansatz for the time-evolving wavepacket was assessed by comparison with converged multiconfigurational (MCTDH) calculations that can be considered as numerically exact. The relevant space of system parameters was explored with respect to the coupling strength as well as the relative timescales of the subsystem and the bath.

In the parameter regimes we considered, the TDH approximation represents a good approximation, i.e., the dynamical evolution is reproduced in a qualitatively correct way, and tunneling rates and yields differ by no more than a factor of two from the exact result. Yet, the quantitative error is non-negligible, such that the error estimates developed in Ref. [3] are relevant. In the present study, this error is numerically computed and compared with our rigorous mathematical estimates [3]. These estimates were shown to provide a good approximation to the numerically exact error, and yield an almost exact result in the early regime of near-linear growth of the error with time before saturation.

Against the background of a detailed scaling analysis, we further introduced a linearization approach by which an expression for the short-time error estimate was derived, which is found to depend on the frequency ratio of the subsystems. This emphasizes that from the vantage point of the TDH approximation, the frequency ratio rather than the mass ratio of the subsystems is of crucial importance. Again, the linearization estimate was found to provide a valid approximation, even beyond the shortest time scale.

The present work paves the way for extensions of error analysis to other types of wavefunction *ansatz*, such as multiconfigurational forms of MCTDH type [1, 6], and especially Gaussian-based hybrid wavefunctions such as employed in the G-MCTDH method [4, 16]. The model that we used showed moderate failures of TDH that have observable consequences on, for example, the reaction probability. It could thus be useful for benchmarking a hierarchy of methods of various sophistication.

**Acknowledgements.** The authors warmly thank Lucien Dupuy, Gérard Parlant, Yohann Scribano and Graham Worth for important discussions and support during the genesis redaction of this article. We thank the CIRM for twice hosting our interdisciplinary team and the CNRS 80prime project for support.

## REFERENCES

- [1] M. Beck, A. Jäckle, G. Worth, and H.-D. Meyer. The multiconfiguration time-dependent Hartree (MCTDH) method: a highly efficient algorithm for propagating wavepackets. *Physics Reports*, 324(1):1–105, 2000.
- [2] P. R. Bunker and P. Jensen. *Molecular symmetry and spectroscopy*. NRC Research Press, Ottawa, 2006.
- [3] I. Burghardt, R. Carles, C. Fermanian Kammerer, B. Lasorne, and C. Lasser. Separation of scales: dynamical approximations for composite quantum systems. *J. Phys. A*, 54(41):Paper No. 414002, 36, 2021.
- [4] I. Burghardt, H.-D. Meyer, and L. S. Cederbaum. Approaches to the approximate treatment of complex molecular systems by the multiconfiguration time-dependent Hartree method. *J. Chem. Phys.*, 111:2927, 1999.
- [5] P. A. M. Dirac. Note on exchange phenomena in the thomas atom. *Mathematical Proceedings of the Cambridge Philosophical Society*, 26(3), 1930.
- [6] F. Gatti, B. Lasorne, H.-D. Meyer, and A. Nauts. *Applications of Quantum Dynamics in Chemistry*. Lectures Notes in Chemistry. Springer International Publishing, 2017.
- [7] R. B. Gerber, V. Buch, and M. A. Ratner. Time-dependent self-consistent field approximation for intramolecular energy transfer: I. Formulation and application to dissociation of van der Waals molecules. *J. Chem. Phys.*, 77:3022, 1982.
- [8] R. B. Gerber and M. A. Ratner. Mean-field models for molecular states and dynamics: new developments. *J. Phys. Chem.*, 92(11):3252–3260, 1988.
- [9] M. Gruebele. Quantum dynamics and control of vibrational dephasing. *J. Phys.: Condens. Matter*, 16:R1057, 2004.
- [10] B. Lasorne, G. Dive, D. Lauvergnat, and M. Desouter-Lecomte. Wave packet dynamics along bifurcating reaction paths. *J. Chem. Phys.*, 118(13):5831–5840, 2003.
- [11] A. M. Levine, M. Shapiro, and E. Pollak. Hamiltonian theory for vibrational dephasing rates of small molecules in liquids. *J. Chem. Phys.*, 88:1959, 1988.
- [12] C. Lubich. *From quantum to classical molecular dynamics: reduced models and numerical analysis*. Zurich Lectures in Advanced Mathematics. European Mathematical Society (EMS), Zürich, 2008.
- [13] H.-D. Meyer, U. Manthe, and L. S. Cederbaum. The multi-configurational time-dependent Hartree approach. *Chem. Phys. Lett.*, 165(1):73–78, 1990.
- [14] H. Nakamura and G. Milnikov. *Quantum Mechanical Tunneling in Chemical Physics*. CRC Press, 1st edition, 2013.
- [15] D. Picconi and I. Burghardt. Open system dynamics using Gaussian-based multi-configurational time-dependent Hartree wavefunctions: Application to environment-modulated tunneling. *J. Chem. Phys.*, 150:224106, 2019.
- [16] S. Römer and I. Burghardt. Towards a variational formulation of mixed quantum-classical molecular dynamics. *Molecular Physics*, 111(22-23):3618–3624, 2013.
- [17] F. Schroeder and A. W. Chin. Simulating open quantum dynamics with time-dependent variational matrix product states: towards microscopic correlation of environment dynamics and reduced system evolution. *Phys. Rev. B*, 93:075105, 2016.
- [18] A. Strathearn, P. Kirton, D. Kilda, J. Keeling, and B. W. Lovett. Efficient non-Markovian quantum dynamics using time-evolving matrix product operators. *Nature Communications*, 9:3322, 2018.
- [19] G. A. Worth, K. Giri, G. W. Richings, I. Burghardt, M. H. Beck, A. Jäckle, and H.-D. Meyer. Quantics package, version 2.0, 2020.

INSTITUTE OF PHYSICAL & THEORETICAL CHEMISTRY, GOETHE UNIVERSITY FRANKFURT, GERMANY

*Email address:* burghardt@chemie.uni-frankfurt.de

UNIV RENNES, CNRS, IRMAR - UMR 6625, F-35000 RENNES, FRANCE

*Email address:* Remi.Carles@math.cnrs.fr

UNIV PARIS EST CRÉTEIL, CNRS, LAMA, F-94010 CRÉTEIL, FRANCE, UNIV GUSTAVE EIFFEL, LAMA, F-77447 MARNE-LA-VALLÉE, FRANCE

*Email address:* clotilde.fermanian@u-pec.fr

ICGM, UNIV MONTPELLIER, CNRS, ENSCM, MONTPELLIER, FRANCE

*Email address:* benjamin.lasorne@umontpellier.fr

TECHNISCHE UNIVERSITÄT MÜNCHEN, ZENTRUM MATHEMATIK, DEUTSCHLAND

*Email address:* classer@ma.tum.de